Springer

KSME

Journal of Mechanical Science and Technology 32 (10) (2018) 5039~5047
www.springerlink.com/content/1738-494x(Print)/1976-3824(Online)
DOI 10.1007/s12206-018-0951-9

Development of a survivability evaluation procedure for bullet penetration into human body †

Gil Ho Yoon[1,*], Ki Hyun Kim[1] and Se Jin Hwang[2]

[1]*School of Mechanical Engineering, Hanyang University, Seoul 04763, Korea*
[2]*Department of Anatomy and Cell Biology, College of Medicine, Hanyang University, Seoul 04763, Korea*

(Manuscript Received February 2, 2018; Revised June 18, 2018; Accepted July 3, 2018)

Abstract

This paper develops survivability evaluation procedure (KUSAR ST-33 program) for bullet penetration into human body based on the AIS (abbreviated injury scale) and the NISS (new injury severity score). Depending on the energy and geometrical configuration of bullet, the shape of temporary wound cavity inside human body is different and this influences the extent of injury. First, some bullet experiments are carried out to extract representative shapes of temporary cavities according to bullet types, and three-dimensional matrix representing human anatomical structure is constructed from scanned CT images of upper body. By mapping the extracted cavity shapes to the 3D matrix for anatomical structure, volume of damaged tissues of some internal organs including blood vessels and bones are calculated. Finally, the AIS and the NISS scores depending on the trajectories of bullets and energy levels are computed with some random variation effects. Bullet trajectories and consequent damaged anatomical structure are visualized.

Keywords: Abbreviated injury scale; Gunshot wound; Human model; New injury severity score; Survivability; Vulnerability simulation

1. Introduction

To determine the type and severity of injuries due to the bullet penetration to human body or gunshot wounds, this paper develops survivability analysis procedure based on the KUSAR ST-33 program, shown in Fig. 1. It is known that, depending on the energy level and the geometrical configurations of bullets, the survivability rate of soldiers with gunshot wound vary statically. For this reason, the temporary and permanent cavities which occur by bullet penetration are different and the damage mechanisms are influenced. The developed 3D injury assessment procedure visualizes the bullet trajectories and temporary cavities inside the human body and provides the survivability score based on the AIS (abbreviated injury scale) by which complex and variable factors related to the survivability are reduced to a single number.

A simulation based computation of the vulnerability and survivability rates of combat soldiers or civilians from penetrating harmful objects is needed in order to estimate the medical response and to predict the outcomes of wounded patients [1-5]. Further, it plays an important role in developing a protecting system or weapons to minimize or maximize hazard injuries [4]. Therefore, some relevant researches have been conducted. A human model simulating the vulnerability of soldiers aboard ships was developed (see Ref. [2] and references therein). In Ref. [6], a mathematical (probabilistic) representation of a conditional survival function was proposed using the tactical medical logistics (TML+) planning tool. There are several studies for the army that simulate the human damages as a result of explosions or high speed impacts [1-5, 7-15]. In addition, some military research centers have been developing several computer programs for the purpose of vulnerability assessment [1-5].

The present KUSAR ST-33 program was developed by following procedures. Firstly, some experiments on ballistic gelatins were conducted to extract the shapes of the internal bullet cavities. Finite element (FE) simulation of bullet penetration was conducted using the viscoelastic material model obtained from the tension test for human cadaver muscle and from the relaxation test for pig organs. Secondly, the cross section images of upper body scanned by a medical CT machine are segmented into numbered pixels and stacked to construct a three-dimensional matrix. Thirdly, the three-dimensional matrix is used to determine the amount of damage of some major organs depending on the bullet trajectory and extracted cavity shapes. Lastly, the AIS (and NISS) scoring system is adopted to get the injury severity and survivability information due to the damaged organs.

The remaining parts are organized as follows. In Sec. 2.1,

*Corresponding author. Tel.: +82 2 2220 0451
E-mail address: ghy@hanyang.ac.kr, gilho.yoon@gmail.com
† Recommended by Associate Editor Yoon Hyuk Kim

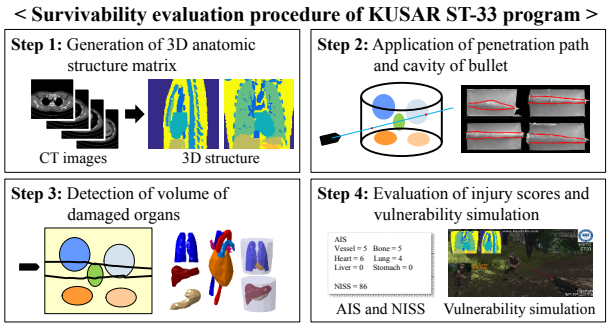

Fig. 1. Four steps of survivability evaluation procedure in KUSAR ST-33 program.

the shapes of temporary cavities of several bullets are extracted from gunshot experiments. In Sec. 2.2, from the CT images of a human body a three-dimensional anatomical structure is established [16-26]. In Sec. 2.3, the bullet trajectory and shape of temporary cavity are defined for 3D anatomical structure to extract the damaged volume of some major organs. In Sec. 2.4, with the help of the AIS (abbreviated injury score) and the NISS (new injury severity score), the injury severity of a human depending on the bullet trajectory and energy is computed. In the example of Sec. 3, several case studies were included to illustrate how the developed procedure predicts tangible outcomes that represent a difference of survivability. Finally, our findings and conclusions are summarized.

2. Survivability analysis for ballistic wounds

2.1 Experiments on bullet penetration

It is impossible to test bullet penetration phenomena directly on humans and there are many limitations in obtaining the related information. Furthermore, some legal and ethical issues exist that involve investigating gun related accidents or criminal firearms discharges. To approximate the internal damages of personnel, we carried out real bullet firing experiments inside 10 % ballistic gelatin blocks, as shown in Fig. 2. With a high speed camera, temporary cavity can be obtained and this information can be regarded as a replication of the damage mechanisms inside personnel with some discrepancies. Information about the shape and characteristics of temporary cavity generated inside gelatin blocks was also collected from relevant Refs. [7, 9, 27, 28]. Depending on the energies and shapes of bullets, not to mention, the energy dissipation mechanisms inside gelatin blocks are different [7, 9, 27, 28]. From our experiments on gelatin block, we witnessed that the overall trajectories of bullets are not significantly altered. We admit that some variations of the penetration trajectory are expected in human body due to the inhomogeneous material properties and the existence of bones and membranous structures. Along the bullet trajectory, some internal organs will be damaged.

Different phenomena are observed from our ballistic gelatin

Bullet	Mass	Velocity	Energy
.22 LR	2.6 g	343 m/s	159 J
.38 Special	10.2 g	290 m/s	420 J
9 mm	7.5 g	352 m/s	462 J
.45 ACP	15.0 g	255 m/s	483 J
.357 Magnum	10.2 g	376 m/s	725 J

(a)

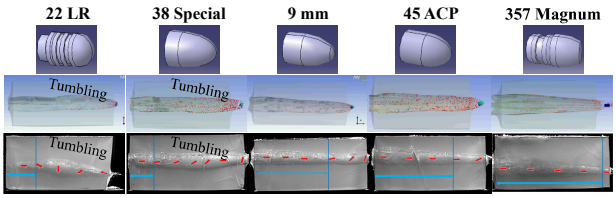

(b)

Fig. 2. (a) Specifications; (b) gun firing simulation and experiment for various bullets.

experiments, depending on the energies and shapes of bullets. The energy of a .22 LR gun with a 2.9 g bullet (projectile) before impact is about 195 J, and inside the ballistic gelatin, the bullet loses some energy and becomes unstable, resulting in some tumbling motion. Just before exit of the 30 cm gelatin block, the bullet rotates 180 degrees. With the tumbling phenomenon, the sizes of temporary cavities are dramatically increased, and from a medical point of view, the corresponding parts of internal organs will be damaged. A .38 special gun has energy of 420 J before impact. This bullet also rotates about 90 degrees inside the gelatin block. A 9 mm bullet with 462 J of impact energy travels several centimeters before it begins tumbling. The 9 mm bullet also rotates 90 degrees before it exits. The .45 ACP bullet with 483 J of impact energy also travels through the gelatin block. Compared with the first three bullets, the .45 ACP bullet has a larger energy. Therefore, it shows little rotation and less tumbling than those of the first three bullets. The .357 Magnum, which has 725 J of pre-impact energy, shows a similar straight trajectory. Even though it has the highest energy, its damage due to the temporary cavity is minimized.

Fig. 3 lists the temporary cavity shapes of the above gunshot experiments [7, 27, 28] in Fig. 2. Depending on different bullet trajectories and different sizes of temporary cavity, the injury scale can be different, which initiated our research. In our analysis, information about various damage mechanisms depending on the type of bullet can be saved in a database and integrated.

2.2 Generation of a 3D anatomical structure matrix

To score the severity of injury by gunshot, the temporary cavity shapes of the various bullets studied in the previous section can be integrated with the 3D anatomical information [16-26]. To achieve this, this research proposes making a 3D anatomical structure matrix from high quality human body CT scans. Although there are many researches for the modeling of

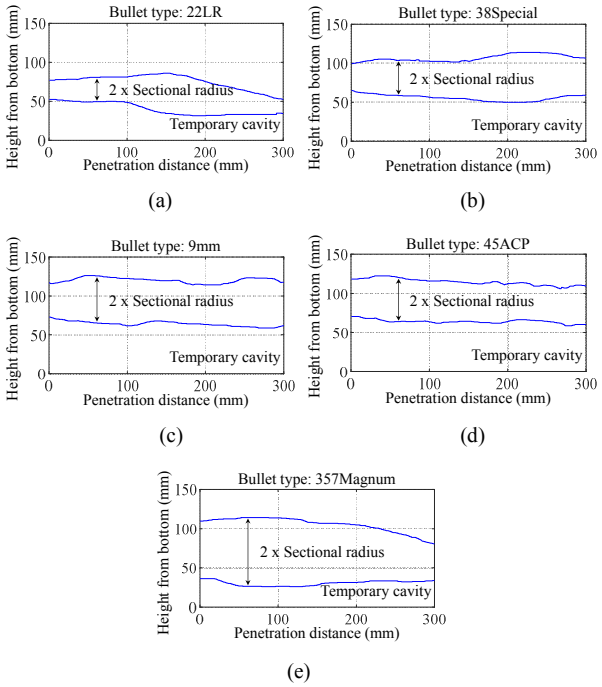

Fig. 3. Extraction of temporary cavity shapes for (a) .22 LR; (b) .38 special; (c) 9 mm; (d) .45 ACP; (e) .357 magnum bullet.

human body feature [29-31] and related application programs using a digital human model [32], researches for the modeling of internal anatomical structure of human body and its application program are not found well. This subsection describes how to construct the 3D anatomical structure matrix implemented in our vulnerability analysis.

The first step of our work is to obtain a set of high quality CT scan images. Medical imaging techniques such as computerized tomography (CT), magnetic resonance imaging (MRI) or ultrasound imaging generate a representation of a patient's anatomy for medical diagnosis [16-26]. For the 3D segmentation of human body, 100 cross section images are taken for the marked region in Fig. 4, as this region is important in computing the injury score. The areas of major vessels, bones, major thoracic and abdominal organs are manually indexed for each CT image, as shown in Fig. 4. The in-plane resolution of indexed pixels is 3.9 mm and the distance between adjacent CT image slices is approximately 3.5 mm. By combining all the indexed pixels of 100 images, we can construct a set of hexahedral voxels with approximated size of 3.7 mm (average of 3.5 mm and 3.9 mm). The pixels for vessel, bone, heart, lung, liver, and stomach are indexed as 1, 2, 3, 4, 5 and 6, respectively. The pixels for the remaining parts are indexed as 9. The pixels out of the body are indexed as 0.

Note that there is little research that considers damage to the vessel part of the anatomy. Following discussion with a medical doctor, it is commented that the injury to the major blood vessels in the chest is an important factor in determining survivability. The major vessels included in the indexed pixels are ascending and descending aorta, aortic arch, thoracic and

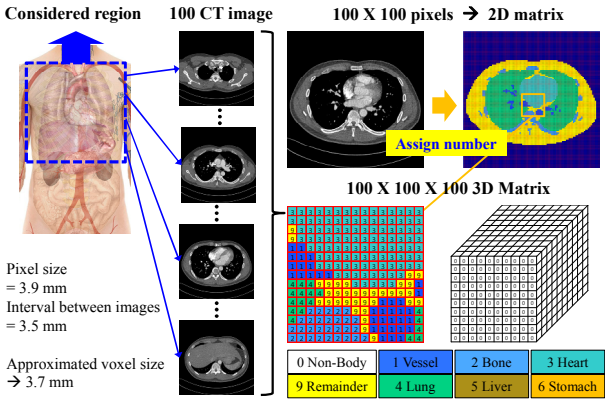

Fig. 4. A 3D anatomical structure obtained from CT images (picture on the left side representing human body is uncopyrighted picture downloaded from https://pixabay.com).

abdominal aorta, brachiocephalic trunk, common carotid artery, subclavian artery, pulmonary trunk, and main branches of the pulmonary artery and pulmonary vein, subclavian vein, internal jugular vein, brachiocephalic vein, superior vena cava and inferior vena cava. The bones included in the index are thoracic and upper lumbar vertebrae, scapula, sternum, ribs.

2.3 Calculation of damaged tissues

We defined the bullet trajectory and temporary cavity shape using the indexed voxels of anatomical structure. The indexed voxels are stored in the form of the three-dimensional matrix. To aid the programming convenience, we used element position of the 3D matrix as coordinates for calculating bullet trajectory. In this case, real-size voxels are mapped into unit-size voxels, as shown in Fig. 5. After that, the bullet trajectory is generated by linear line defined by the two points, i.e., an impact point and an exit point. With the bullet firing information provided by a user, it is possible to consider the various directions of bullet penetrations.

The cavity shapes from the gunshot experiments in Sec. 2.1 are mapped along the bullet trajectory line. Furthermore, the two idealized shapes, i.e., parabolic and semi parabolic shapes, can be implemented by a user definition. Following discussions with researchers for the Republic of Korea Army, some random irregularities in the bullet trajectory and the cavity size are implemented with the "rand" matlab function. A user can define a maximum perturbed distance from the straight trajectory as shown in Fig. 10(b). This maximum perturbed distance and the sum of six sine (or cosine) functions with random frequencies generated by the "rand" matlab function are used to generate random disturbances. In addition, a user can define a maximum radius increase of temporary cavity. This value is also multiplied to a random value between 0 and 1 also generated by the "rand" matlab function.

Now, assuming that the tissues of internal organs inside the cavities are damaged, the indexes of the voxel elements within the cavity are extracted and used to calculate the volume of

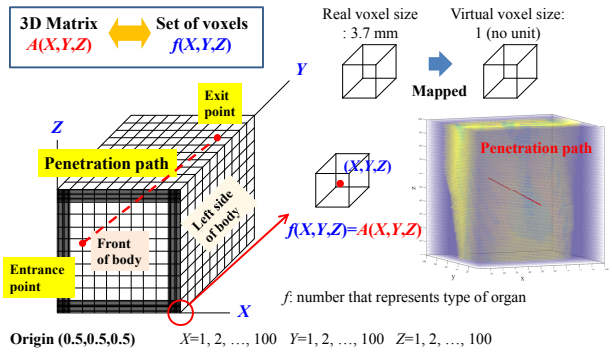

Fig. 5. Definition of bullet trajectory in 3D matrix of anatomical structure.

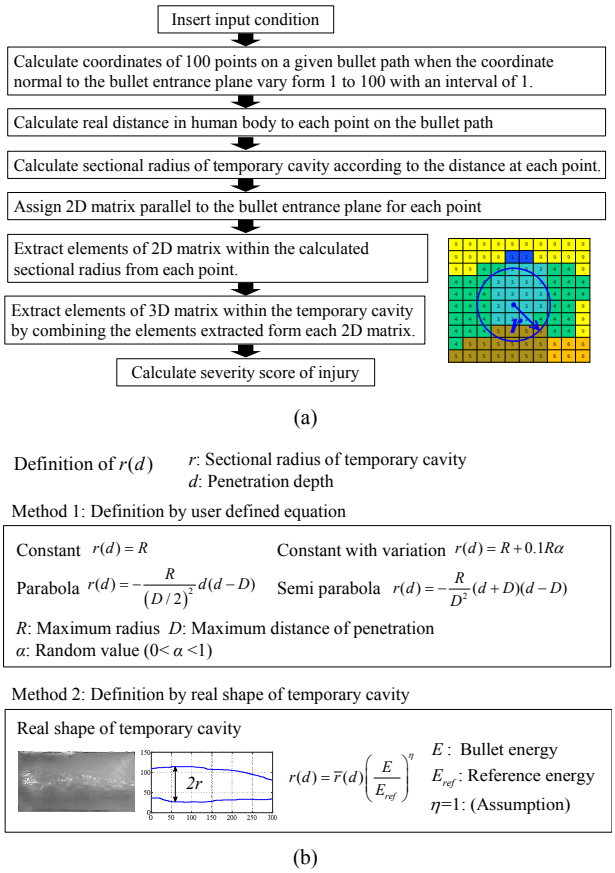

Fig. 6. (a) Flowchart of the damage computing algorithm; (b) the radius modeling of temporary cavities (idealized parabola and semi parabola shapes and the cavity shapes from experiments).

damaged tissues for each indexed organ. The overall calculation procedure for 3D matrix is illustrated in Fig. 6(a). Some mathematical algorithms are developed to extract the indexes of the voxel elements within the cavity defined by Fig. 6(b).

2.4 Application of injury scoring system (AIS and NISS)

The computed volume of damaged internal organs is scored using the abbreviated injury scale (AIS) and the new injury

AIS Score	Description
1	Minor
2	Moderate
3	Serious
4	Severe
5	Critical
6	Maximal

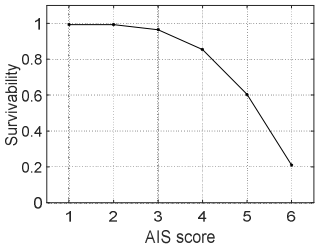

Fig. 7. The abbreviated injury scale system and the survivability rate according to the AIS score.

severity score (NISS) systems [8-15, 27, 33-36]. The AIS is an anatomy based scoring system developed by the Association for the Advancement of Automotive Medicine (AAAM) in order to classify and describe the severity of injuries and estimate the survivability. Based on statistical approaches, the threat to life associated with the injury can be digitized. The AIS is a widely used anatomical scale for traumatic injuries. It has been revised since 1969 with major updates. In the AIS system, we can see numbers, which vary from 1 to 6, as shown in Fig. 7. The injury cases with AIS Score 1 are minor injuries and the injury cases with AIS Score 6 are untreatable injuries.

With the AIS system, the new injury severity score (NISS) can be computed as a measure of injury severity for patients with multiple traumas. The NISS (new injury severity score) is the sum of the squares of the three largest values of the AIS scores regardless of body region. Compared to the NISS, the original ISS (injury severity score) is the sum of the squares of the highest AIS scores for the three most severely injured body regions. In the calculation of the ISS, body regions are divided into six regions (head or neck, face, thorax, abdomen, extremities and external). But as expected, it is not enough to summarize the injury severity of a patient with multiple traumas with a single number. So in emergency centers, various scoring systems such as the revised trauma score (RTS), the acute physiology and chronic health evaluation (APACHE), the trauma score-injury severity score (TRISS), or a severity characterization of trauma (ASCOT) are used.

The AIS score for each organ is computed depending on the damage rate of each organ (defined by the damaged volume per the total volume) as Table 1. For instance, whether the damaged volume of the vessel parts is below 5 % of the total vessel volume or not, the AIS score is set to 5 or 6. In the similar way, the AIS scores of the other organs are calculated according to the criteria of Table 1 which is a quantitatively simplified version of the original AIS score originally developed in the framework of KUSAR ST-33. Then, the square sum of the three largest values among the AIS scores of individual organs is defined as the NISS score. The anatomical structure inside cavity is visualized in the present KUSAR ST-33 program, as shown in Fig. 8. The sectional views (top, right, and front views) are represented. Fig. 9 shows the entire process of the developed program.

Table 1. Criteria for AIS score decision from the damage rate of each organ (D: Damage rate (%)).

Vessel	$0 < D < 5$	$5 \le D \le 100$	
AIS score	5	6	
Bone	$0 < D < 15$	$15 \le D \le 100$	
AIS score	4	5	
Heart	$0 < D < 5$	$5 \le D \le 100$	
AIS score	5	6	
Lung	$0 < D < 25$	$25 \le D < 50$	$50 \le D \le 100$
AIS score	3	4	5
Liver	$0 < D < 25$	$25 \le D < 50$	$50 \le D \le 100$
AIS score	3	4	5
Stomach	$0 < D < 15$	$15 \le D < 50$	$50 \le D \le 100$
AIS score	2	3	4

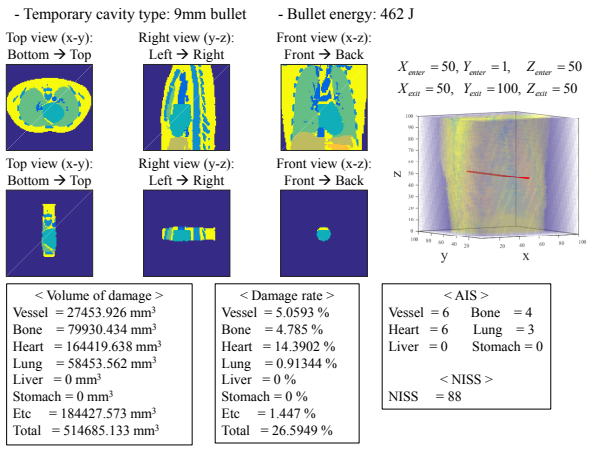

Fig. 8. An AIS score computing example.

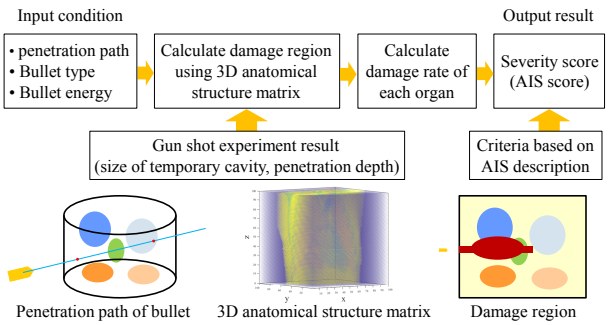

Fig. 9. The AIS computation procedure.

3. Damage simulation examples

This section shows some simulation results with the developed procedure (KUSAR ST-33). The program computes different AIS and NISS scores depending on the impact points and the energies of different bullets related to the size of temporary cavity.

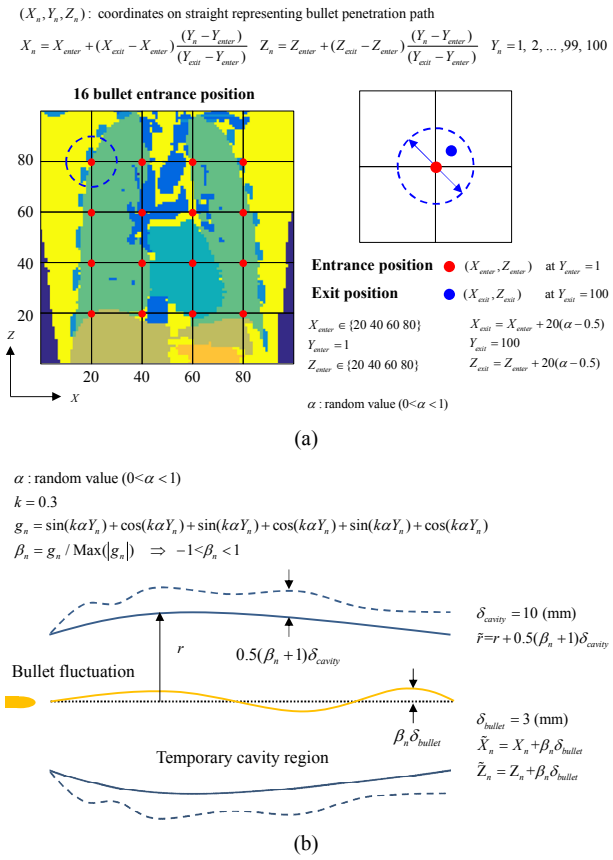

Fig. 10. An example of calculating the survivability due to the front gun shot: (a) Illustration of entrance and exit position of bullet; (b) random variation of bullet trajectory and radius of temporary cavity.

3.1 Example 1: Survivability analysis of front gunshot

For the first example, the gunshot impact on 16 points of the chest is considered as Fig. 10. We assumed that bullets have sufficient energies and penetrate the body almost perpendicularly. The variations of the exit position of bullet and the fluctuations of the bullet trajectory and the radius of temporary cavity are included with randomness in Fig. 10(b). The bullet exit position can be any point inside the circle with radius of 10 units (10×3.7 mm=3.7 cm). It is controlled by a random parameter α . For the smooth variations of bullet trajectory and radius of temporary cavity, six sine functions (or cosine functions) are summed whose frequencies are randomly chosen. These random characteristics were included to consider the environmental factors such as soldier proficiency, wind, target movement and the resistance factors inflicted to bullet. Some additional random variations can be modeled, but this has not been implemented in the present program. Furthermore, to overcome current limitations and improve the accuracy of the program, real combat data should be inserted.

Fig. 11 shows the computed mean AIS and the mean NISS scores with a 9 mm bullet with 462 J of energy for 16 points. To obtain the mean scores, 100 bullet penetration simulations are carried out for each impact point. As mean AIS score is

Table 2. AIS mean score and NISS mean score of the first example (Fig. 11).

Position (x,y)	AIS (mean)						NISS (mean)
	Vessel	Bone	Hear-t	Lung	Liver	Stom-ach	
(20,20)	0.40	4.00	0.00	3.00	3.00	0.00	35.28
(20,40)	2.90	4.00	0.00	3.00	0.00	0.00	39.50
(20,60)	1.50	4.00	0.00	3.00	0.00	0.00	32.50
(20,80)	5.00	4.00	0.00	3.00	0.00	0.00	50.00
(40,20)	5.03	4.00	5.20	3.00	3.00	0.00	68.53
(40,40)	5.57	4.00	5.78	3.00	0.00	0.00	80.85
(40,60)	6.00	4.00	4.10	3.00	0.00	0.00	74.12
(40,80)	5.42	4.00	0.00	3.00	0.00	0.00	54.62
(60,20)	5.06	4.00	6.00	3.00	3.00	0.91	78.05
(60,40)	5.69	4.00	6.00	3.00	0.00	0.00	84.59
(60,60)	6.00	4.00	5.27	3.00	0.00	0.00	79.97
(60,80)	5.90	4.00	0.00	3.00	0.00	0.00	59.90
(80,20)	1.25	4.00	5.01	3.00	3.00	0.30	54.89
(80,40)	4.80	4.00	3.88	3.00	0.00	0.00	61.65
(80,60)	4.30	4.00	0.00	3.00	0.00	0.00	46.50
(80,80)	5.00	4.00	0.00	3.00	0.00	0.00	50.00

Table 3. The standard deviations of the AIS and the NISS scores of the first example (Fig. 11).

Position (x,y)	AIS (STD, standard deviation)						NISS (STD)
	Vessel	Bone	Hear-t	Lung	Liver	Stom-ach	
(20,20)	1.36	0.00	0.00	0.00	0.00	0.00	4.36
(20,40)	2.48	0.00	0.00	0.00	0.00	0.00	12.40
(20,60)	2.30	0.00	0.00	0.00	0.00	0.00	11.51
(20,80)	0.00	0.00	0.00	0.00	0.00	0.00	0.00
(40,20)	0.17	0.00	0.40	0.00	0.00	0.00	5.38
(40,40)	0.50	0.00	0.42	0.00	0.00	0.00	6.52
(40,60)	0.00	0.00	1.93	0.00	0.00	0.00	6.18
(40,80)	0.50	0.00	0.00	0.00	0.00	0.00	5.46
(60,20)	0.60	0.00	0.00	0.00	0.00	1.05	3.86
(60,40)	0.46	0.00	0.00	0.00	0.00	0.00	5.11
(60,60)	0.00	0.00	0.45	0.00	0.00	0.00	4.91
(60,80)	0.30	0.00	0.00	0.00	0.00	0.00	3.32
(80,20)	2.18	0.00	0.78	0.00	0.00	0.72	9.17
(80,40)	0.98	0.00	2.14	0.00	0.00	0.00	10.08
(80,60)	1.74	0.00	0.00	0.00	0.00	0.00	8.72
(80,80)	0.00	0.00	0.00	0.00	0.00	0.00	0.00

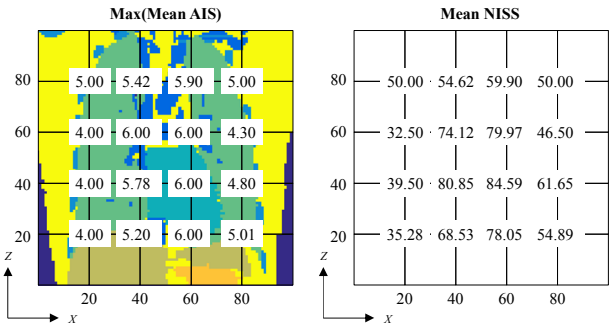

Fig. 11. The survivability computation for 9 mm bullet with 462 J of energy.

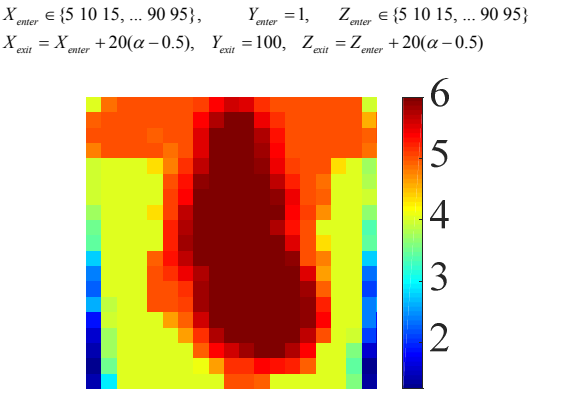

Fig. 12. Visualization of the detailed survivability computation for 9 mm bullet with 462 J of energy.

computed for an individual organ, the mean score shown in Fig. 11 is maximum score among the organs. As expected, the AIS score near the heart and the main blood vessel parts above the heart is 6, which is the highest score of the AIS scoring system. Due to this high score, the ballistic wound near the heart is very fatal and instant death is expected. When this bullet impacts near the left side area, i.e., (20,20), (20,40) or (20,60), the score is reduced to 4. This score is due to the fact that the important organs such as heart, major vessels are far from the side. When the impact point moves to the right side between 40 and 60, the score increases, as expected. The NISS score shows the similar tendency. Tables 2 and 3 give the detailed values for the scores. Because random parameters are used, there are few statistical variations for the repeated simulation.

Fig. 12 shows the refined AIS score distribution of Fig. 11. From this information, survivability of some wounded soldiers can be predicted by observing the positions of penetration wounds although bullet energies of different kinds of weapons should be considered as following examples.

Fig. 13 shows that the AIS score and the NISS score when the energy of a 9 mm bullet is decreased to a half and a quarter of the initial value, respectively. Here, it is also assumed that the radius of temporary cavity linearly decreases with respect to the impact energy of bullet. Reduction of bullet energy can be considered when the distance between the gun and body increases. The NISS score near the heart at (60, 60) is significantly decreases from 79.97 to 73.69 and 60.69 while the NISS score at (20, 20) slightly decreases from 35.28 to 33.64 and 32.65. Therefore, the results in Figs. 11 and 13 imply that the extent of change of survivability rate according to the bullet energy varies for different impact points.

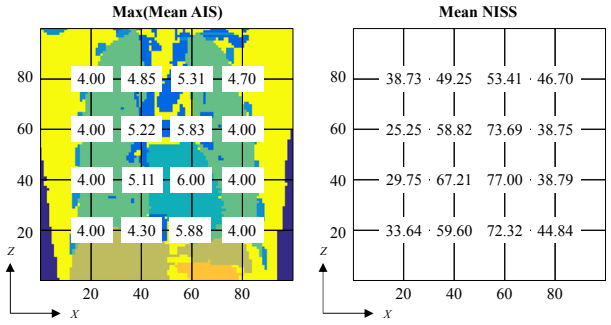

Fig. 13. The survivability computation (using the formulation in Fig. 6(b)) for a 9 mm bullet with (a) 231 J (a half of the energy of Fig. 11); (b) 115.5 J (a quarter of the energy of Fig. 11).

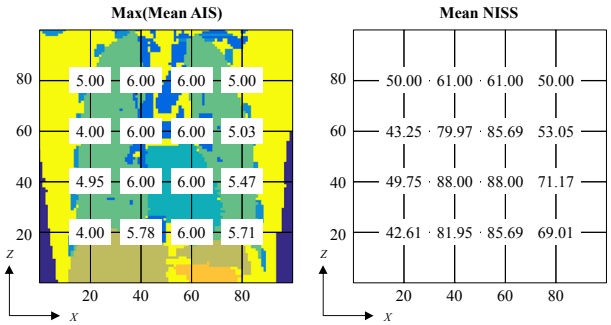

Fig. 14. The survivability computation for (a) .357 magnum bullet (725 J); (b) .22LR bullet (159 J).

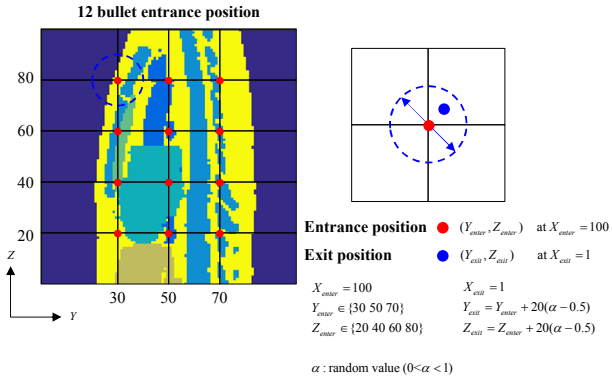

Fig. 15. An example of calculating the survivability due to the side gun shot.

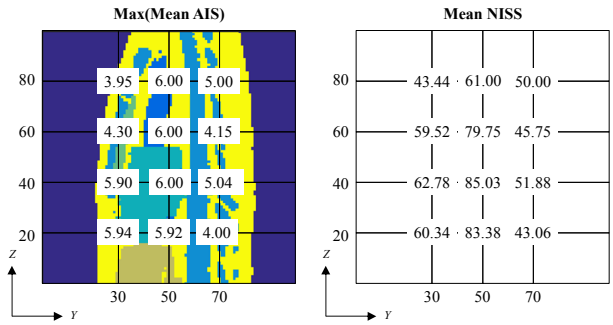

Fig. 16. The survivability computation for 9 mm bullet with 462 J of energy (side gunshot).

Fig. 14(a) shows the computed AIS score and the NISS score with a .357 Magnum bullet with 725 J of energy. Note that the shape in Fig. 3 is used in the calculation of scores. Because of the high dynamic energy of the bullet, the AIS and the NISS scores increase. The NISS score at (20, 20) also increases significantly by 7 points. Fig. 14(b) shows the mean AIS score and the mean NISS score for a .22LR bullet with 159 J of energy. Because of relatively low energy, the overall scores are smaller than those of a 9 mm bullet. But the injury is still fatal near the heart.

3.2 Example 2: Survivability analysis of side gunshot

As a next example, the survivability rate for the side gunshot is computed with a 9 mm bullet of 462 J in Fig. 15. The 12 positions are considered assuming the penetration through the body model. The random variations for exit position, bullet trajectory and radius of temporary cavity are also implemented as previous examples.

Fig. 16 shows the varying survivability rates for the side gunshot depending on the impact point. The mean AIS and NISS scores increase when bullet impacts near the important organs such as heart, major blood vessels and decrease when bullet impacts far from the internal organs. In addition to this example, a further sophisticated situation can be simulated considering various gunshot situations.

4. Conclusions

This research presents a survivability evaluation procedure for gunshot wounds for the application of Republic of Korea Army or police. This research was initiated as a part of a long-term research to recognize and identify relevant items of information for human survivability. In order to develop a unified survivability model for Korea, some missing and unclear information are independently researched and they are integrated into the unified survivability program KUSAR ST-33 [37, 38]. In this regard, damage mechanism by bullet penetration was investigated by gunshot experiments with 10 % gelatin blocks whose behaviors are known to be similar to those of human muscle. Depending on the energy and the shape of bullets, the shapes of temporary cavities inside human body are different. The temporary cavity shapes for gelatin block are extracted for various bullets and are integrated with the 3D anatomical structure for which internal organs were numbered with different indexes. We assumed that the damaged tissues inside temporary cavity influence the survivability and computed the AIS and NISS injury scores related to survivability rate depending on the trajectory of bullet. In short, this research developed a survivability analysis procedure by the combination of gunshot experiment results and 3D anatomical structure matrix. For further research on this topic, it is necessary to verify the computed survivability rate with real damage cases and include vital signs.

Acknowledgments

This work was supported by the research fund of Survivability Technology Defense Research Center of Agency for Defense Development of Korea (No. UD150013ID) and Institute of Civil Military Technology Cooperation of Korea (No. UM16201RD2 “Development of smart alternative equipment with appropriate physical power”).

References

[1] D. N. Neades and E. G. Davis, A new approach to the simulation of battlefield injuries and their effect on the performance of military tasks, *20th International Conference on Ballistics*, Orlando, FL (2002).

[2] B. Jacobs, L. A. Young, D. H. Champion, M. Lawnick, D. M. Galarneau, V. Wing and D. W. Krebs, Applying modeling and simulation to predict human injury due to a blast attack on a shipboard environment, *Proceedings of the Human Factors and Ergonomics Society Annual Meeting*, 56 (1) (2012) 2359-2363.

[3] M. Aberdeen, *Operational requirements-based casualty assessment: ORCA user's manual*, Army Research Laboratory (2008).

[4] E. Natalie and G. Patrick, *Survivability analysis for the evaluation of personnel in body armor*, Army Reearch Laboratory (2010).

[5] M. M. Lawnick, H. R. Champion, T. Gennarelli, M. R. Galarneau, E. D'Souza, R. R. Vickers, V. Wing, B. J. Eastridge, L. A. Young, J. Dye, M. A. Spott, D. H. Jenkins, J. Holcomb, L. H. Blackbourne, J. R. Ficke, E. J. Kalin and S. Flaherty, Combat injury coding: A review and reconfiguration, *J. Trauma Acute Care*, 75 (4) (2013) 573-581.

[6] R. Mitchell, M. Galarneau, B. Hancock and D. Lowe, *Modeling dynamic casualty mortality curves in the tactical medical logistics (TML+) planning tool*, Navl Health Research Center (2004).

[7] C. Amy and C. Michael, *Physical mechanisms of soft tissue injury from penetrating ballistic impact*, U.S. Air Force Academy (2012).

[8] H. Ceylan, A. McGowan and M. D. Stringer, Air weapon injuries: a serious and persistent problem, *Arch Dis Child*, 86 (4) (2002) 234-235.

[9] J. S. Denton, A. Segovia and J. A. Filkins, Practical pathology of gunshot wounds, *Arch Pathol Lab Med*, 130 (9) (2006) 1283-1289.

[10] Z. Duric, I. Gosev and D. Belina, Penetrating injury to the right side of the heart without hemodynamic compromise, *J Thorac Cardiov Sur*, 144 (1) (2012) 263-264.

[11] J. W. Finnie, Forensic pathology of traumatic brain injury, *Vet Pathol*, 53 (5) (2016) 962-978.

[12] A. D. Levy, R. M. Abbott, C. T. Mallak, J. M. Getz, H. T. Harcke, H. R. Champion and L. A. Pearse, Virtual autopsy: Preliminary experience in high-velocity gunshot wound victims, *Radiology*, 240 (2) (2006) 522-528.

[13] N. Maiden, Ballistics reviews: mechanisms of bullet wound trauma, *Forensic Sci Med Pat*, 5 (3) (2009) 204-209.

[14] W. R. Nemzek, S. T. Hecht, P. J. Donald, R. A. McFall and V. C. Poirier, Prediction of major vascular injury in patients with gunshot wounds to the neck, *Am J Neuroradiol*, 17 (1) (1996) 161-167.

[15] M. Oehmichen, C. Meissner, H. G. Konig and H. B. Gehl, Gunshot injuries to the head and brain caused by low-velocity handguns and rifles: A review, *Forensic Sci Int*, 146 (2-3) (2004) 111-120.

[16] M. J. Ackerman, The visible human project: A resource for education, *Acad Med*, 74 (6) (1999) 667-670.

[17] J. S. Park, M. S. Chung, S. B. Hwang, Y. S. Lee, D. H. Har and H. S. Park, Visible Korean human: Improved serially sectioned images of the entire body, *IEEE T Med Imaging*, 24 (3) (2005) 352-360.

[18] S. X. Zhang, P. A. Heng, Z. J. Liu, L. W. Tan, M. G. Qiu, Q. Y. Li, R. X. Liao, K. Li, G. Y. Cui, Y. L. Guo, X. P. Yang, G. J. Liu, J. L. Shan, J. J. Liu, W. G. Zhang, X. H. Chen, J. H. Chen, J. Wang, W. Chen, M. Lu, J. You, X. L. Pang, H. Xiao, Y. M. Xie and J. C. Y. Cheng, The Chinese visible human (CVH) datasets incorporate technical and imaging advances on earlier digital humans, *J. Anat*, 204 (3) (2004) 165-173.

[19] M. S. Chung and S. Y. Kim, Three-dimensional image and virtual dissection program of the brain made of Korean cadaver, *Yonsei Med J.*, 41 (3) (2000) 299-303.

[20] H. S. Hwang, J. G. Shin, B. H. Lee, T. J. Eom and C. K. Joo, In vivo 3D meibography of the human eyelid using real time imaging Fourier-domain OCT, *Plos One*, 8 (6) (2013).
[21] D. S. Shin, J. S. Park, H. S. Park, S. B. Hwang and M. S. Chung, Outlining of the detailed structures in sectioned images from Visible Korean, *Surg Radiol Anat*, 34 (3) (2012) 235-247.
[22] L. Tang, M. S. Chung, Q. A. Liu and D. S. Shin, Advanced features of whole body sectioned images: Virtual Chinese human, *Clin Anat*, 23 (5) (2010) 523-529.
[23] J. S. Park, Y. W. Jung, J. W. Lee, D. S. Shin, M. S. Chung, M. Riemer and H. Handels, Generating useful images for medical applications from the visible Korean human, *Comput Meth Prog Bio*, 92 (3) (2008) 257-266.
[24] J. F. Uhl, J. S. Park, M. S. Chung and V. Delmas, Three-dimensional reconstruction of urogenital tract from visible Korean human, *Anat Rec Part A*, 288A (8) (2006) 893-899.
[25] V. Spitzer, M. J. Ackerman, A. L. Scherzinger and D. Whitlock, The visible human male: A technical report, *J. Am Med Inform Assn*, 3 (2) (1996) 118-130.
[26] V. M. Spitzer and D. G. Whitlock, The visible human dataset: The anatomical platform for human simulation, *Anat Rec*, 253 (2) (1998) 49-57.
[27] P. M. Rhee, E. E. Moore, B. Joseph, A. Tang, V. Pandit and G. Vercruysse, Gunshot wounds: A review of ballistics, bullets, weapons, and myths, *J. Trauma Acute Care*, 80 (6) (2016) 853-867.
[28] L. F. Martin, *Wound ballistics research of the past twenty years: A giant step backwards*, Letterman Army Institute of Research (1990).
[29] C. C. L. Wang, T. K. K. Chang and M. M. F. Yuen, From laser-scanned data to feature human model: A system based on fuzzy logic concept, *Comput Aided Design*, 35 (3) (2003) 241-253.
[30] I. F. Leong, J. J. Fang and M. J. Tsai, Automatic body feature extraction from a marker-less scanned human body, *Comput Aided Design*, 39 (7) (2007) 568-582.
[31] S. Y. Zhu, P. Y. Mok and Y. L. Kwok, An efficient human model customization method based on orthogonal-view monocular photos, *Comput Aided Design*, 45 (11) (2013) 1314-1332.
[32] J. Z. Yang, J. H. Kim, K. Abdel-Malek, T. Marler, S. Beck and G. R. Kopp, A new digital human environment and assessment of vehicle interior design, *Comput Aided Design*, 39 (7) (2007) 548-558.
[33] R. A. Santucci and Y. J. Chang, Ballistics for physicians: Myths about wound ballistics and gunshot injuries, *J Urology*, 171 (4) (2004) 1408-1414.
[34] S. A. Padosch, P. H. Schmidt and B. Madea, Planned complex suicide by self-poisoning and a manipulated blank revolver: Remarkable findings due to multiple gunshot wounds and self-made wooden projectiles, *J. Forensic Sci*, 48 (6) (2003) 1371-1378.
[35] N. Maiden, Historical overview of wound ballistics research, *Forensic Science, Medicine, and Pathology*, 5 (2) (2009) 85-89.
[36] C. Xu, Y. B. Chen, B. C. Li, L. C. Zhang, J. M. Wang, J. Y. Kang, Z. Q. Chen and X. X. Li, Finite element analysis vs experimental study of head firearm wound in pig, *Technol Health Care*, 23 (2015) S61-S70.
[37] N. R. Park, K. H. Kim, J. S. Mo and G. H. Yoon, An experimental study on the effects of the head angle and bullet diameter on the penetration of a gelatin block, *Int. J. Impact Eng.*, 106 (2017) 73-85.
[38] G. H. Yoon, J. S. Mo, K. H. Kim, C. H. Yoon and N. H. Lim, Investigation of bullet penetration in ballistic gelatin via finite element simulation and experiment, *Journal of Mechanical Science and Technology*, 29 (9) (2015) 3747-3759.

Gil Ho Yoon received his B.S. degree in mechanical and aerospace engineering from Seoul National University in 1998. And he received his M.S. and Ph.D. degrees in mechanical and aerospace engineering from Seoul National University in 2000 and 2004, respectively. Dr. Yoon is currently a Professor at School of Mechanical Engineering, Hanyang University, Seoul, Republic of Korea.

Ki Hyun Kim received his B.S. degree in mechanical engineering from Hanyang University in 2013. Mr. Kim is currently an Ph.D. candidate at Department of Mechanical Convergence Engineering, Hanyang University, Seoul, Republic of Korea.

Se Jin Hwang received his B.S. degree in medicine from Hanyang University in 1987. And he received his M.S. and Ph.D. degrees in medicine from Hanyang University in 1989 and 1995, respec-tively. Dr. Hwang is currently a Professor at College of Medicine, Hanyang University, Seoul, Republic of Korea.